Original Article | Journal of Biosystems Engineering

J. of Biosystems Eng. 39(3):174-183. (2014. 9)
http://dx.doi.org/10.5307/JBE.2014.39.3.174

eISSN : 2234-1862
pISSN : 1738-1266

Automatic Extraction of Lean Tissue for Pork Grading

Sung-ho Cho[1], Le Ngoc Huan[2], Sun Choi[3], Tae-Jung Kim[4], Wu-hyun Shin[4], Heon Hwang[4]*

[1]Agri. Machinery Certification Team, Foundation of Agri. Tech. Commercialization & Transfer, 22, Suin-ro 135beon-gil, Gwonseon-gu, Suwon-si, Gyeonggi-do, 441-857, Korea
[2]Robotics Lab, Simla, Agaworld Bldg. 279 Gangnam-daero, Seocho-gu, Seoul, 137-862, Korea
[3]USDA, ARS. Russell Research Center 950 College Station Road Athens, GA 30605, USA
[4]Department of Bio-Mechatronic Engineering, College of Biotechnology & Bioengineering, Sungkyunkwan University, 300 Chunchun, Jangan, Suwon, Gyeonggi, 440-746, Korea

Received: July 11st 2014; Revised: August 9th 2014; Accepted: August 20th 2014

Abstract

Purpose: A robust, efficient auto-grading computer vision system for meat carcasses is in high demand by researchers all over the world. In this paper, we discuss our study, in which we developed a system to speed up line processing and provide reliable results for pork grading, comparing the results of our algorithms with visual human subjectivity measurements. **Methods:** We differentiated fat and lean using an entropic correlation algorithm. We also developed a self-designed robust segmentation algorithm that successfully segmented several porkcut samples; this algorithm can help to eliminate the current issues associated with autothresholding. **Results:** In this study, we carefully considered the key step of auto-extracting lean tissue. We introduced a self-proposed scheme and implemented it in over 200 pork-cut samples. The accuracy and computation time were acceptable, showing excellent potential for use in online commercial systems. **Conclusions:** This paper summarizes the main results reported in recent application studies, which include modifying and smoothing the lean area of pork-cut sections of commercial fresh pork by human experts for an auto-grading process. The developed algorithms were implemented in a prototype mobile processing unit, which can be implemented at the pork processing site.

Keywords: Adaptive segmentation, Color Computer Vision (CCV), Entropic correlation, Pork grading

Introduction

The pork industry has made significant progress in recent years in altering the composition of carcasses, resulting in fresh cuts and processed products to provide consumers with meat products that are leaner, with less trimmable fat. This strong positive progress in product composition has allowed the industry to shift more attention to another important feature of pork, the quality of the lean. "Lean quality" in fresh pork can refer to a wide range of factors, such as color, water holding capacity, marbling, flavor, drip loss, tenderness, and pH, but in this study we will focus on such factors as muscle color, texture, and marbling. These factors affect the product's attractiveness to potential customers, the processing characteristics for value-added product manufacturing, and the ultimate palatability and satisfaction of pork products to consumers.

At this time, development and installation of a system for instrumental assessment of the value of a pork carcass is critical in Korea because livestock producers are not sufficiently confident in the current subjective grading system of animal products (Kim et al., 2007). As an alternative to the current grading system, color computer vision (CCV) holds promise for obtaining quality measurements, such as accuracy, efficiency, acceptability, and processing time. This novel method also has the benefit of removing the human subjectivity that is associated with visual

***Corresponding author:** Heon Hwang
Tel: +82-31-290-7825; **Fax:** +82-31-290-7825
E-mail: bionuke@hanmail.net

measurements.

The value of a pork carcass is determined by the size and quality of the tissue area. Therefore, extracting the contour of the lean-tissue is not only essential but should be the first step for precise evaluation of the pork carcass value. However, the algorithm used for the rapid and robust separation of the lean tissue from the mixture of lean and fat tissue in pork cuts has considerable problems. Because the boundary of lean tissue is sometimes very complex and obscure, it is very difficult to distinguish clearly its boundary.

In image processing, one of the most efficient technologies for image segmentation is entropy-based thresholding. This approach uses the Shannon entropy—which originated from information theory—and considers the gray level image histogram, two-dimensional (2D) histogram, or co-occurrence matrix as a probability. The entropic approach for image segmentation can be divided into two methods: *global* and *local*. The global method associates the entire image with a single threshold value by using the gray level histogram of the image. In Portes de Albuquerque et al. (2004), the Tsaillis entropy, a novel approach to generate the Boltzmann/Gibbs's traditional entropy, was introduced as a new method of image segmentation. Subsequently, minimum cross entropy thresholding, used by Yin et al. (2007), Pal et al. (1996), and Brink et al. (1996), was developed as a novel approach for segmenting an image. Normally, measurements made using entropic methods were based on the image itself, its histogram, or other related distributions, assuming that the pixels within the image were independent of each other. Meanwhile, Brink (1996) showed that when a combination of the spatial information and maximum entropy were considered, using context-related information can drastically improve the results; such information is available at little additional computational cost. In addition, Sahoo et al. (1997) presented a general technique using global thresholding methods to threshold digital images based on Renyi's entropy.

It is generally believed that image processing naturally bears some fuzziness. The fuzzy cpartition entropy approach for threshold selection behaves well in segmenting images. A number of studies on fuzzy entropy methods were reported by Cheng et al. (1998), Liu et al. (2006), Tao et al. (2003), and Tao et al. (2007). However, the size of the search space increased very rapidly when the number of parameters needed to determine the membership function increased. Consequently, the time needed for fuzzy entropy methods is an obstacle for realtime targets. A 2D entropy thresholding algorithm that used the 2-D entropies based on the 2-D—gray level and local average gray level—histogram to segment images was presented by Wu et al. (1999), Sahoo et al. (2004), Feng et al. (2004), and Jansing et al. (1999).

In contrast, the local method partitions a given image into a number of sub-images and determines a threshold for each sub-image. Recently, a newly developed local segmentation method based upon a transition region was introduced by Yan et al. (2003). Although global and local methods can be applied successfully to segment image samples of a pork cut, the local method seems to require much more computing time for an image with a size of 640 x 480 pixels or larger.

In this paper, we discuss a maximum correlation criterion for bi-level thresholding (Yen et al., 1995), which provides the best results in accuracy and rapidity among the algorithms described previously. The main objective of this research was to develop algorithms that automatically extract a contour of the lean tissue boundary as closely and robustly as possible to the result of a human grading expert. A heuristic approach was also used to estimate the lean tissue contour. The results achieved so far are significant and this technique seems promising as a steady auto grading system for commercial pork carcasses. We also developed a prototype mobile pork quality measurement system, which can be implemented at the pork processing site. The developed system was composed of a handheld image acquisition unit and a mobile processing unit. The algorithms developed in this study were implemented in the mobile processing unit as a supplementary grading device.

Materials and Methods

Mobile image processing unit

Using the developed mobile image acquisition and processing unit, we collected sample images of pork sections at the Hannaeng Company, Korea cold storage, in Seoul. The developed mobile unit was composed of a handheld image acquisition unit (Figure 1) and a mobile computing unit mounted with a 17" Notebook (Figure 1). A ring type white LED indirect lighting device (LFR130-SW, CCS Inc., Japan) and CCD camera (CV-735, Jai, Japan) were assembled

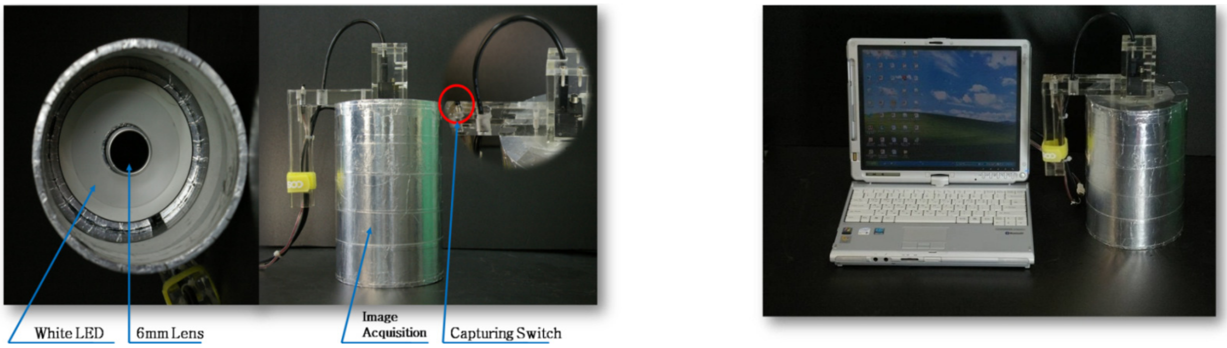

Figure 1. Handheld image acquisition device.

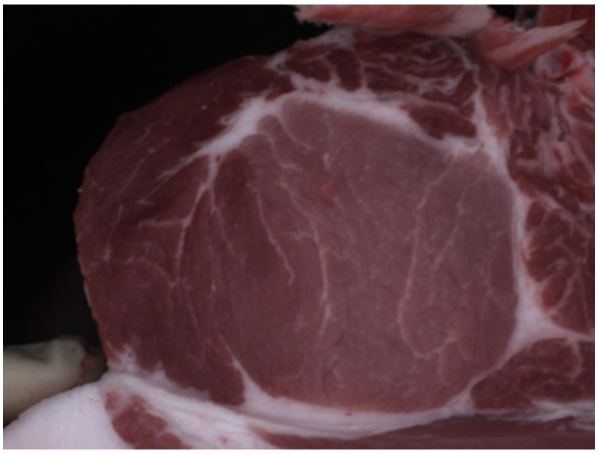

Figure 2. Image obtained using the handheld image acquisition device.

as a cap shape. Figure 2 shows an image obtained using the handheld image acquisition device. We made the measurement and analysis software with Visual Basic 6.0.

Lean tissue segmentation

Because the colors of the lean tissue and fat are different for each carcass, depending on carcass quality, automatic lean-tissue segmentation is not a simple process. In order to overcome the difficulties of the segmentation caused by the color variation of the lean tissue, the auto-thresholding algorithm using the entropic correlation method was applied to the green frame of the acquired input image. The image of the pork captured from CCV was in the Red, Green, and Blue (RGB) format. Selecting a proper color band that best reflects the features of the image was crucial in the segmentation process. The image from the green channel was chosen as a reference because it was most appropriate to histogrambased segmentation.

Consider an image $f(x, y)$ of size N x N pixels that are represented by m gray-levels. Let Gm {0, 1,. . ., (m - l)} denote the set of gray levels, and f_i, $i \in Gm$ be the observed gray level frequencies of the image f. The probability of the gray level i in the image f can be calculated as

$$p_i = \frac{f_i}{N \times N}, i \in G_m \quad (1)$$

Hence, a distrbution $\{p_i \mid i \in G_m\}$ can be obtained. For a given gray level t, if $\Sigma_{t=0}^{t-1} p_i$ is larger than zero and smaller than one, then the following two distributions can be derived from this distribution after normalization:

$$A_1 \equiv \frac{p_0}{p(t)}, \frac{p_1}{p(t)}, \cdots, \frac{p_{t-1}}{p(t)}$$
$$A_2 \equiv \frac{p_t}{1-p(t)}, \frac{p_{t+1}}{1-p(t)}, \cdots, \frac{p_{m-1}}{1-p(t)}$$

where $p(t) = \Sigma_{i=0}^{t-1} p_i$ is the total probability up to the *(t - 1)-th* gray level.

The entropic correlation method was proposed by Yen et al. (1995) and given by defining

$$C_X(t) = -\ln \Sigma_{i \geq 0} p_i^2 \quad (2)$$

where X is a discrete random variable with a finite or countable infinite range $R = x_0, x_1, x_2, \ldots$ and p_i is the probability of $X = x_i$. In the maximum entropy criterion, the basic idea is to choose the threshold such that the total amount of information provided by the object and background is maximized. The correlation provided by the classes A_1 and A_2 can be calculated based on the previous definition. The correlations associated with the distributions A_1 and A_2 are defined

$$C_{A_1}(t) = -\ln \Sigma_{i=0}^{t}\left(\frac{p_i}{p(A_1)}\right)^2 \quad (3)$$

$$C_{A_2}(t) = -\ln \Sigma_{i=t+1}^{255}\left(\frac{p_i}{1-P(A_1)}\right)^2 \quad (4)$$

respectively. The total available correlation, which will be denoted by *TC*, provided by A_1 and A_2 is

$$\begin{aligned} TC(t) &= C_{A_1}(t) + C_{A_2}(t) \quad (5)\\ &= -\ln \Sigma_{i=0}^{t}\left(\frac{p_i}{P(A_1)}\right)^2 - \ln \Sigma_{i=t+1}^{255}\left(\frac{p_i}{1-P(A_1)}\right)^2 \\ &= -\ln\left(\frac{G_{A_1}(t)\,G_{A_2}(t)}{P(A_1)^2(1-P(A_1))^2}\right) \\ &= -\ln\left(G_{A_1}(t)\,G_{A_2}(t)\right) + 2\ln\left(P(A_1)(1-P(A_1))\right) \end{aligned}$$

where,

$$G_{A_1}(t) = \Sigma_{i=0}^{t} p_i^2 \quad (6)$$

$$G_{A_2}(t) = \Sigma_{i=t+1}^{255} p_i^2 \quad (7)$$

We use the maximum entropy criterion to determine the threshold t* such that

$$TC(t^*) = max_{t \in G_m}\, TC(t) \quad (8)$$

Finding the lean tissue area of pork section

Filtering small blobs

We merged the fat parts after the thresholding scheme had been implemented. The small blobs that sometimes affect the identification of the main lean contour should be first filtered out. As seen in Gonzalez and Woods (2002), a labeling algorithm, also called "extraction of connected components," can group and sum the number of pixels connected to each other. Hence, in this study, a blob-labeling process was applied to the threshold image using 8connectivity to filter the fat blobs of the pork that contained a low number of pixels.

Finding the central point

The boundary between the fat and lean tissue areas in the pork carcass was still not clearly visible. After obtaining firm, significant fat blobs—see Figure 3(a)—and after applying the bloblabeling process to the threshold image, locating the relative position of the center of the main lean tissue part, surrounded by discrete fat blobs, is crucial to generating the desired lean tissue area. In this study, we moved a specific circle throughout the entire image to find a space that contained a large number of circles with or without any fat tissue inside. We then saved the position of the centers of these circles. Subsequently, a centroid was approximately generated by interpolating from the positions of the circles, as Figure 3(b) shows.

Searching main points on the boundary

The algorithm found the *spine points* of the boundary connecting the fat blobs by moving a specific quarter of an earring shape that departed from the centroid—see Figure 3(c)—to four sides of the image, with a difference of 10° for each iteration. While moving in an arbitrary direction from the centroid, the algorithm saved either the position of the first contact point between the earring shape and the fat blob in the direction of movement, and scanned the other path; or it met the pixel position at the side of the image and the process would begin in successive directions. If the circle reached the edges of the image, the algorithm ignored the position of these points.

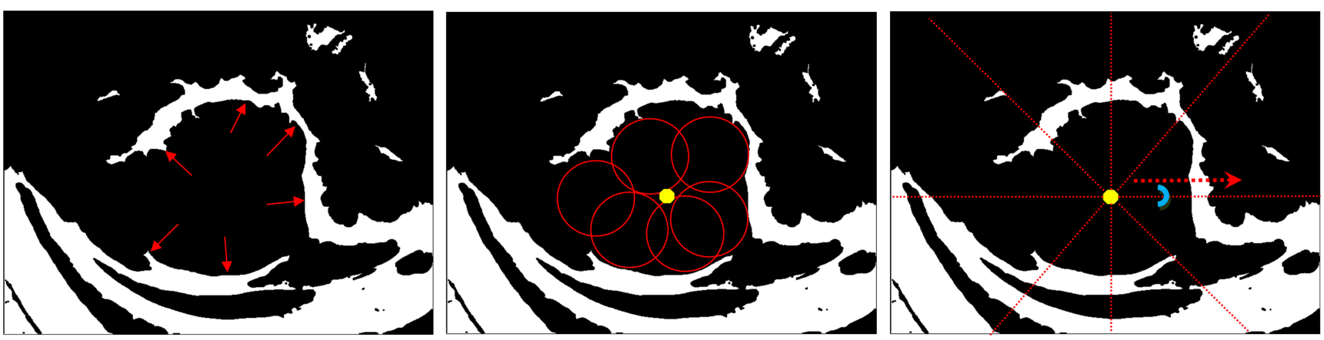

(a) (b) (c)

Figure 3. Obtaining spine points: (a) Fat regions used for searching the centroid; (b) The centroid; (c) Finding spine points.

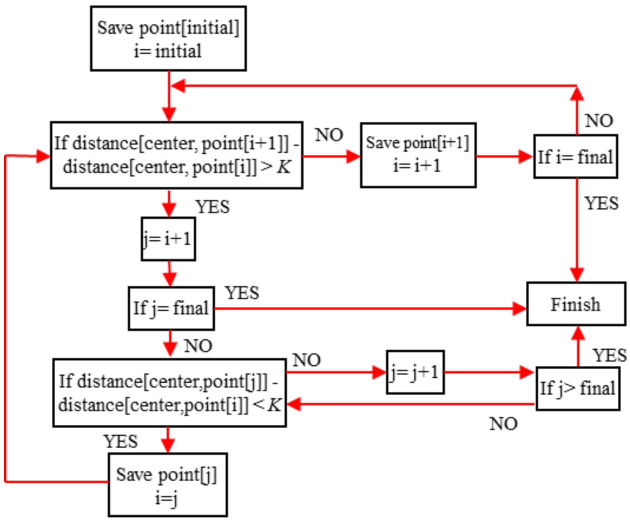

Figure 4. Flowchart of the algorithm used to detect the main points.

In order to locate the correct contour containing only the lean part of the carcass, the algorithm analyzed the respective positions of the determined spine points in detail to discard unnecessary points and to keep the qualified points as needed. At first, the shortest distance from the center to the points was determined and used as an initial point. We then implemented this process in two directions—counterclockwise and clockwise. In each direction, a set of two points, including the current one and the upcoming points, were considered successively. Figure 4 briefly describes this algorithm.

In this algorithm, *K* is a positive coefficient that was estimated from practice based upon the number of determined spine points—in this study, 36—and the actual shape of the desired lean tissue area—normally, a circle or ellipse. We used a *K* value of 25 pixels.

Iterative contour modification

The remaining spine points were directly connected to generate a contour of the lean tissue area. However, in practice, there were some concave valleys that existed along the contour because of extraneous portions of the fat regions. A human expert decides on the lean tissue contour by considering the composition pattern of the fat and the loin regions based on experience. Automatic extraction of lean tissue contour should, to a certain degree, have the ability to mimic the process that a human expert uses. Portions of the contour having extreme changes in curvature were assumed to be deep valleys and these irregularities were eliminated using the following algorithm. Further details of this algorithm are in the study published by Huan et al. (2009).

First, by using the Overhauser curve generation scheme, a temporary shape of the lean part was generated via the remaining spine points. The Overhauser curve C(t) that can generate a curve while satisfying the 2nd derivative continuity was generated by

$$C(t) = [a][b][c] \tag{9}$$

where, $[a] = [t3, t2, t, 1]$;

$$[b] = \begin{vmatrix} -0.5 & 1.5 & -1.5 & 0.5 \\ 1 & -2.5 & 2 & -0.5 \\ -0.5 & 0 & 0.5 & 0 \\ 0 & 1 & 0 & 0 \end{vmatrix}, [c] = \begin{vmatrix} p1 \\ p2 \\ p3 \\ p4 \end{vmatrix}$$

Parameter *t* varies from 0 at p_2 to 1 at p_3 with the step of 0.1 (t = 0, 0.1, 0.2 … 1). We use the four successive remaining spine points, p_1, p_2, p_3, and p_4, to generate a curve for the segment between two points, p_2 and p_3.

The boundary of the lean tissue was then extracted from the temporary shape of the lean part using line tracing based on the 8-directional chain coding. By tracing along the temporary boundary and comparing the gradient of each pixel, convex points were found. The algorithm measured the distance between each pair of adjacent convex peaks, as well as the number of pixels between adjacent convex peaks. In order to determine whether or not to modify each segment of the contour between the two convex peaks, we introduced an evaluation function.

In this function, if the total number of pixels in each segment between adjacent convex peaks was greater than a positive constant *K1* multiplied by the distance of two adjacent convex peaks, the segment of the contour between two adjacent peaks was removed and a new contour was generated using the Overhauser curve generation scheme. The value of the positive constant *K1* could determine how much of the deep fat valley was adjusted into the lean tissue portion. We used a default value of 1.2 for *K1*. If a segment between two adjacent peaks, p_2 and p_3 from the Overhauser curve, was a deep fat valley that needed to be modified, p_1 and p_4 were specified along the contour with 30 pixels before p_2 and after p_3, respectively.

After segment modification was carried out, new concave points were detected and eliminated among the previous peak points. An evaluation function was applied again for

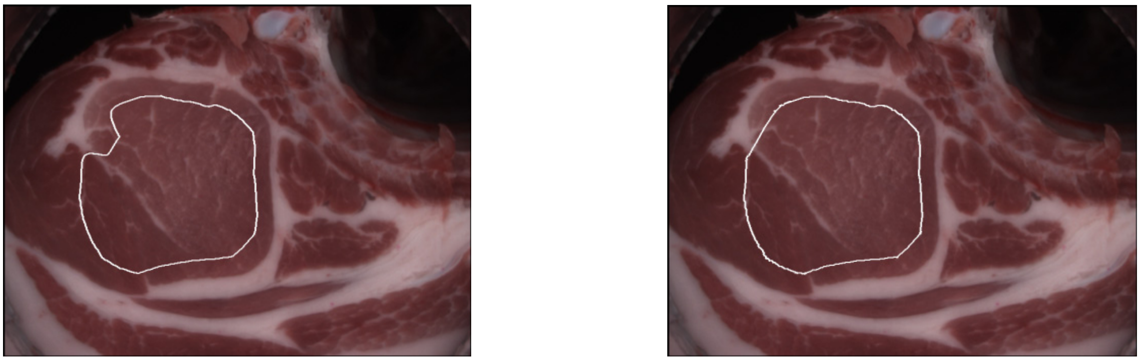

(a) (b)

Figure 5. Concave modification: (a) Before modification; (b) After modification.

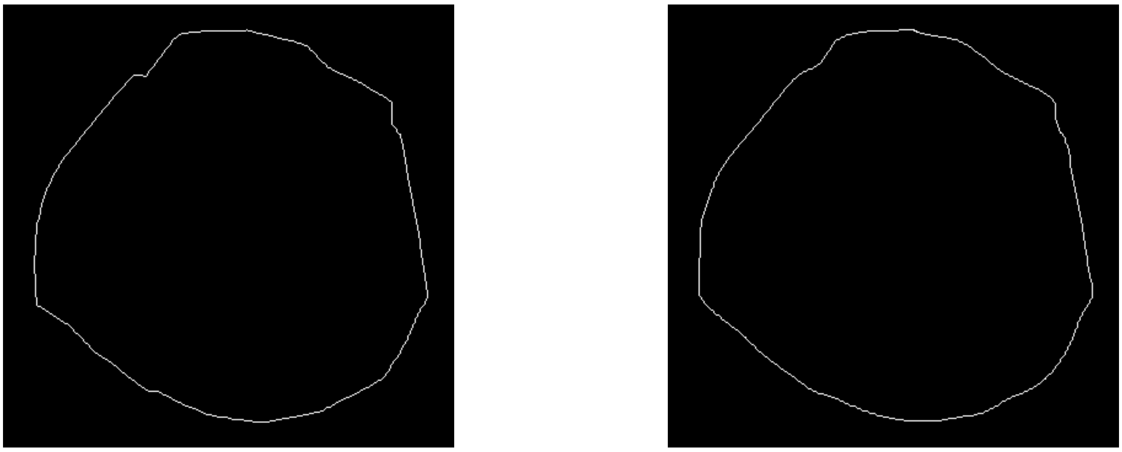

(a) (b)

Figure 6. Smoothing process: (a) Contour before smoothing; (b) Contour after smoothing.

the remaining peaks to determine if the segment required modification or not. This process was carried out iteratively until no more concave points were found.

We achieved the major advantage of this process, precise control over contour modification, using local convex peaks, while maintaining the 2nd derivative of the continuity for the new curve. The modification algorithms could be simply adjusted to mimic the human expert by varying the *K1* value.

Figure 5(b) shows the result after applying the modification algorithm to the temporary shape of the lean part; see Figure 5(a).

Contour smoothing

In general, the extracted contour of the lean-tissue was jagged because of the pixel-based accuracy of the processing algorithm, and so it varied slightly from the result of the human expert, which was a smooth curve. The boundary determined by a human expert was smooth overall in curvature and did not display the jagged features observed in the computed boundary. The jagged boundary was smoothed using a cubic spline, for further details refer to a previous study published by Huan et al. (2009). Figure 6(a) shows the original image and Figure 6(b) shows the resulting image after the boundary smoothing algorithm was applied.

Results and Discussion

Lean tissue segmentation

Using the adaptive thresholding algorithm based on the entropic correlation method—see Figure 7(a)—we used image with the information from the green channel to separate the image into lean and fat tissue, Figure 7(b) shows the result of the lean segmentation process.

The white part is fat tissue and the rest is lean.

(a) (b)

Figure 7. Image segmentation: (a) Raw image; (b) After segmentation.

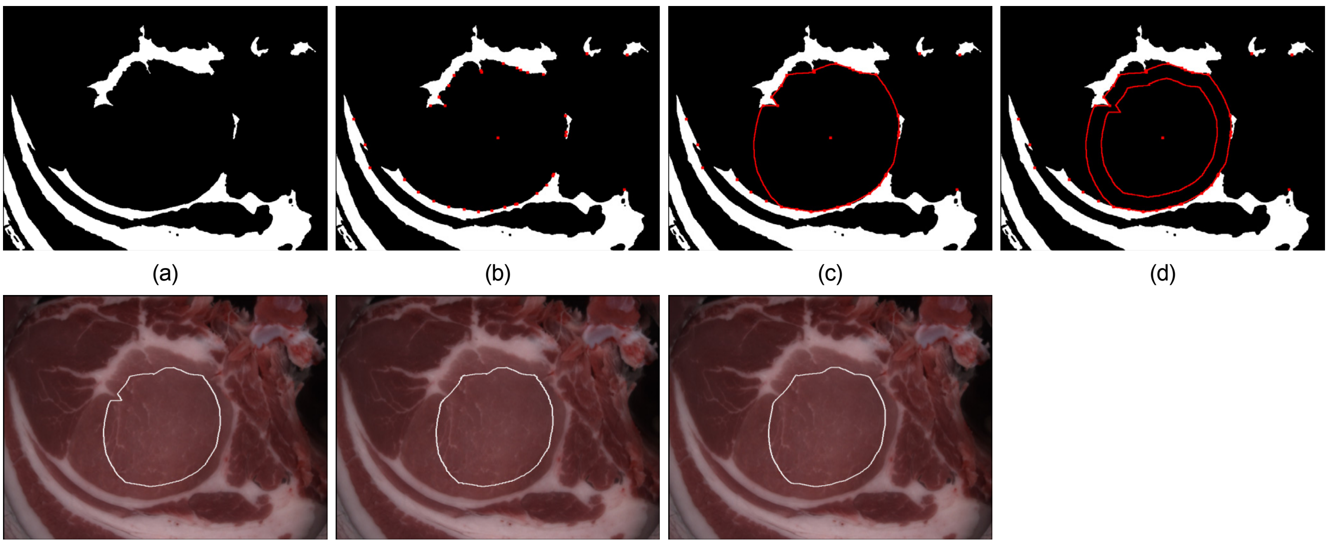

(a) (b) (c) (d) (e) (f) (g)

Figure 8. Results of the boundary extraction process: (a) Image after blobs-labeling; (b) Searching spine points; (c) Generating the temporary contour after omitting unnecessary points; (d) Scaling the temporary contour to 20%; (e) Boundary with a deep valley on the left; (f) After modification process; (g) Smoothing and superimposing onto the raw image.

Finding lean tissue area of pork section

To begin the process of finding the main area of lean tissue, the blob-labeling algorithm removed the small fat blobs from the segmented image; see Figure 8(a). In Figure 8(b), the red point in the center of the image is the centroid that was found by moving the specific circle over the image and interpolating the positions of circles that have no fat parts inside. We then implemented a self-designed algorithm for choosing qualified points to generate the main shape of the lean tissue area and obtained a successful contour; see Figure 8(c). Because the color of the lean tissue region adjacent to the discrete fat parts could not be reliably estimated due to the mixing of the colors of the fat and lean part, the main contour was modified with a 20% scaling operation by using the centroid point and the generated contour. The main contour of lean area extracted from the previous algorithm was superimposed on the original image, as Figure 8(d) shows. In Figure 8(e), a deep concave valley appeared and remarkably changed the curvature of the boundary on the left. We implemented the modification algorithm containing the correction process that uses the Overhauser curve generation scheme, resulting in a smooth added segment, which was as smooth as the one that the human expert created, see Figure 8(f). Finally, the contour was smoothed and superimposed on the original image to validate the result of the boundary extraction process, as Figure 8(g) shows.

In order to select qualified points from a set of initially

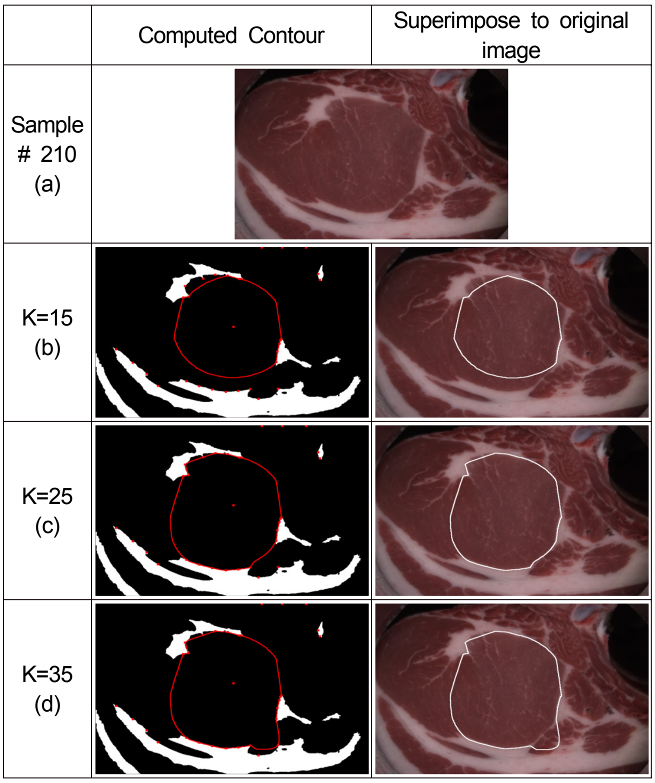

Figure 9. Effects of *k* on contour modification (1): (a) Original image; (b) $k = 15$ and superimposed image; (c) $k = 25$ and superimposed image; (d) $k = 35$ and superimposed image.

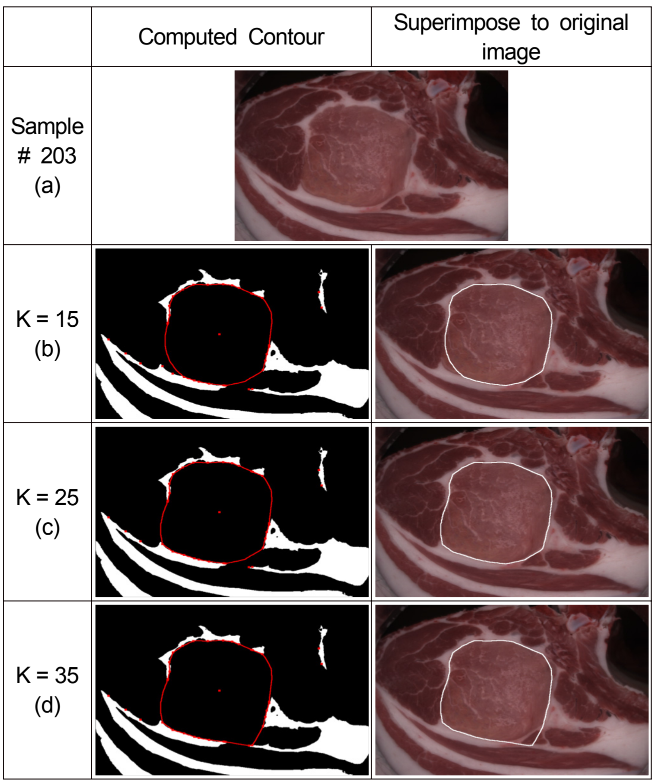

Figure 10. Effects of *k* on contour modification (2): (a) Original image; (b) $k = 15$ and superimposed image; (c) $k = 25$ and superimposed image; (d) $k = 35$ and superimposed image.

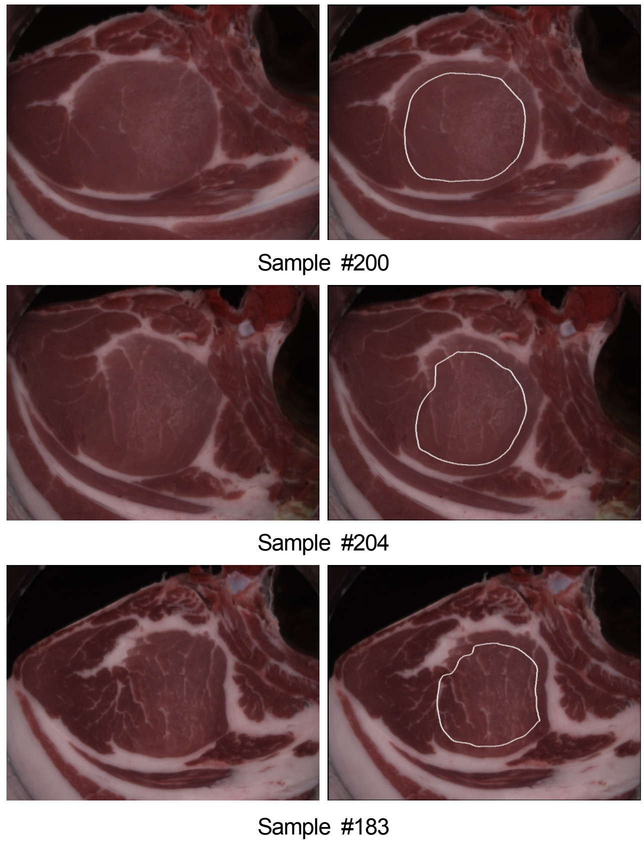

Figure 11. Typical images.

determined spine points, the constant K was carefully selected to generate a boundary that satisfied the boundary obtained by the human expert in almost all of the samples. Figures 9 and 10 show the effects of various values of K on the contour modification. When K was increased, the size of the lean tissue became larger and included undesired lean parts. The default value of K was set to 25 pixels, based on the results obtained from a large number of experiments; we used this value throughout the process.

The developed algorithm was applied to over 200 pork section samples. Figure 11 shows typical images of the contour, which were extracted automatically using the proposed algorithms.

Conclusions

Contour extraction of lean tissue is critical for evaluating pork quality in an automatic manner. Based on the extracted contour, the size and color of the loin, and the marbling state, we can determine the fat composition ratio of lean tissue. In this study, we developed algorithms to automatically extract the boundary of the lean tissue such that the extracted boundary was similar to the one determined by human experts. Image acquisition and processing were implemented in a mobile handheld pork image processing unit. We applied the developed algorithms to over 200 pork-cut samples and obtained successful results for all pork cuts with either moderate or complex patterns of lean tissue. The computing time for contour extraction was approximately 3 seconds, which qualifies as an auto-grading system. In addition, we developed a prototype mobile pork quality measurement system, which can be implemented at pork processing sites.

We found that the algorithms developed for automatic lean tissue contour extraction with a mobile handheld system were good enough to provide the basis for a supplementary tool for the automatic grading of pork quality. The results were acceptable and this method seems promising as an auto real-time online grading method for pork carcasses.

Further studies will quantify color estimation, marbling index, and fat thickness, with the goal of creating an automatic, robust, and efficient mobile system to assess pork quality grade that can be a full substitute for visual measurements by human experts.

Conflict of Interest

The authors have no conflicting financial or other interests.

Acknowledgement

This research was funded by the MAF-SGRP (Ministry of Agriculture and Forestry-Special Grants Research Program) in Korea.

References

Benabdelkader, S., Boulemden, M., Enabdelkader, S and M. Boulemden. 2005. Recursive algorithm based on fuzzy 2-partition entropy for 2-level image thresholding. Pattern Recognition 38:1289-1294.

Brink, A. D and N. E. Pendock. 1996. Minimum cross-entropy threshold selection. Pattern Recognition, 29(1):179-188.

Brink, A. D. 1996. Using spatial information as an aid to maximum entropy image threshold selection. Pattern Recognition letters 17:29-36.

Cheng, H. D., Chen, J. R and J. G. Li. 1998. Threshold selection based on fuzzy c-Partition entropy approach. Pattern Recognition, 31(7):857-870.

Feng, D., Wenkang, S., Liangzhou, C., Yong, D and Z. Zhenfu. 2005. Infrared image segmentation with 2-D maximum entropy method based on particle swarm optimization (PSO). Pattern Recognition Letters 26: 597-603.

Fleury, M., Hayat, L and A. F. Clark. 1996. Parallel entropic auto-thresholding. Image and Vision Computing 14: 247-263.

Gonzalez, R. C and R. E. Woods. 2002. Digital Image Processing. 2nd ed. Reading, Mass: Addison-Wesley.

Huan, L. N., Choi, S., Cho, S. I., Lee, M. H and H. Hwang. 2009. Automatic extraction of lean-tissue contours for beef quality grading. Biosystems Engineering, 102:251-264.

Jansing, E. A. D., Albert, T. A and D. L. Chenoweth. 1999. Two-dimensional entropic segmentation. Pattern Recognition Letters 20:329-336.

Kim, J. H., Choi, S., Han, N. Y., Ko, M. J., Cho, S. H., Hwang, H., Quantization and Calibration of Color Information From Machine Vision System for Beef Color Grading. J of Biosystems Eng. 32(3):160-165.

Liu, D., Jiang, Z and H. Feng. 2006. A novel fuzzy classification entropy approach to image thresholding. Pattern Recognition letters 27:19681975.

Pal, N. R. 1996. On minimum cross-entropy thresholding. Pattern Recognition, 29(4):575580.

Portes de albuquerque, M., Esquef, I. A and A. R. Gesualdi mello. 2004. Image thresholding using Tsaillis entropy. Pattern Recognition letters 25:1059-1065.

Sahoo, P. K and G. Arora. 2004. A thresholding method based on two-dimensional Renyi's entropy. Pattern Recognition 37:1149-1161.

Tao, W. B., Tian J. W and J. Liu. 2003. Image segmentation by three-level thresholding based on maximum fuzzy entropy and genetic algorithm. Pattern Recognition letters 24:3069-3078.

Tao, W., Jin, H and L. Liu. 2007. Object segmentation using ant colony optimization algorithm and fuzzy entropy. Pattern Recognition Letters 28:788-796.

Wu, X. J., Zhang, Y. J and L. Z. Xia. 1999. A fast recurring two-dimensional entropic thresholding algorithm.

Pattern Recognition 32:2055-2061.

Yan, C., Sang, N and T. Zhang. 2003. Local entropy-based transition region extraction and thresholding. Pattern Recognition letters 24:2935-2941.

Yen, J. C., Chang, F. J and S. Chang. 1995. A new criterion for automatic multilevel thresholding. IEEE Trans. Image Process 4:370-378.

Yin, P. Y. 2007. Multilevel minimum cross entropy threshold selection based on particle swarm optimization. Applied Mathematics and Computation 184:503-513.